

# Cyclic voltammetric studies of nickel hydroxide and cobalt hydroxide thin films in alkali and alkaline earth metal hydroxides

P. VISHNU KAMATH, M. F. AHMED

*Department of Chemistry, Central College, Bangalore University, Bangalore 560001, India*

Received 6 May 1992; revised 31 July 1992

Cyclic voltammetric studies of thin films of electrosynthesized (ES)-Ni(OH)<sub>2</sub> and Co(OH)<sub>2</sub> in different alkaline electrolytes suggest that the mechanism of oxidation is different from the mechanism of reduction. While the metal ion (alkali or alkaline earth metal) intercalation–deintercalation from the electrolyte into the film provides the driving force, the reduction reaction takes place heterogeneously independent of the electrolyte concentration, whereas oxidation takes place homogeneously across a nebulously defined electrode–electrolyte interphase. ES-Ni(OH)<sub>2</sub> permits facile intercalation–deintercalation of alkali metal ions Li<sup>+</sup>, Na<sup>+</sup> and K<sup>+</sup>, irrespective of their ionic size, while the reactions of ES-Co(OH)<sub>2</sub> are sensitive to ionic size, requiring larger potentials in KOH compared to LiOH. In the alkaline earth metal hydroxides, both Ni(OH)<sub>2</sub> and Co(OH)<sub>2</sub> films show greater reversible characteristics in the order Ba(OH)<sub>2</sub> > Sr(OH)<sub>2</sub> > Ca(OH)<sub>2</sub>. This may be trivially related to the order of the solubilities of the three hydroxides.

## 1. Introduction

A number of structural [1–3] and electrochemical studies [4,5] have established, with some certainty, that the oxidation–reduction reactions of Ni(OH)<sub>2</sub> and other oxide electrodes such as MnO<sub>2</sub> proceed via an intercalation–deintercalation mechanism. Consequently, electrosynthesized (ES) oxide/hydroxide phases, which are disordered on account of ‘chaotic nucleation’ during electrosynthesis, display a higher electrochemical activity compared to well formed chemically synthesized crystalline phases. These disordered phases are highly hydrated and include large tunnels and intersheet spaces within their structure enabling intercalation and deintercalation of protons [4], alkali metal ions [5], oxo-anions [6] and also hydroxyl ions [7]. The intercalation–deintercalation mechanism has also been extended to explain the oxidation–reduction reactions of Co(OH)<sub>2</sub> [3,8–9].

Of particular interest has been the uptake of alkali metal ions by the active electrode material from the electrolyte. A number of papers report the influence of the electrolyte on the electrode performance.  $\alpha$ -Ni(OH)<sub>2</sub> incorporates alkali metal ions in its bulk lattice while  $\beta$ -Ni(OH)<sub>2</sub> does not [10]. Li<sup>+</sup> readily incorporates into Ni(OH)<sub>2</sub>, substituting for H, but the discharge ends at a higher oxidation state than in KOH [1] resulting in a lower charge capacity. In a recent paper, Vazquez and others [11] have reported a higher discharge efficiency for the Ni(OH)<sub>2</sub> electrode in KOH compared to NaOH and LiOH.

It is thus evident that the alkali metal ion plays a crucial role in determining such important parameters

of battery performance as charge capacity, discharge efficiency and reversible potential. In order to explore this area further the present cyclic voltammetric (CV) investigation of ES-nickel and cobalt hydroxide films was undertaken in a number of alkali and alkaline earth metal hydroxides. In contrast to earlier studies [10], CV enables the independent estimation of the oxidation as well as the reduction reaction potentials and throws light on their mechanism. Further within certain limitations, CV enables us to estimate [12] various parameters such as charge capacity, coulombic efficiency and the reversible potential. The present study indicates that the electrolyte plays a major role in the oxidation and reduction reactions of the oxide electrodes and the mechanism of oxidation is quite different from that of reduction.

## 2. Experimental details

### 2.1. Preparation of thin films

Nickel hydroxide and cobalt hydroxide thin films were deposited on a platinum flag (surface area 1.5 cm<sup>2</sup>) from their respective nitrate solutions (0.1 M), by a one-step cathodic process [13] galvanostatically, at a current density of 1 mA cm<sup>-2</sup>, in an undivided electrolytic cell. The deposition times were 20 s for Ni(OH)<sub>2</sub> and 80 s for Co(OH)<sub>2</sub>. Prior to each deposition the Pt substrate was washed with detergent, concentrated nitric acid and then electrochemically cleaned as described elsewhere [12]. The freshly prepared films were rinsed with water and used for CV studies.

## 2.2. Preparation of electrolyte

Solutions of AnalaR grade LiOH, NaOH and KOH were prepared and pre-electrolysed as described elsewhere [14] for 72 h and then standardized for use in CV experiments. Alkaline earth metal hydroxides have poor solubility and near saturated solutions were prepared for the present study. The solutions used were  $\text{Ca}(\text{OH})_2$ , 0.03 M;  $\text{Sr}(\text{OH})_2$ , 0.09 M;  $\text{Ba}(\text{OH})_2$ , 0.1 M. These were used as such without pre-electrolysis.

## 2.3 Cyclic voltammetry studies

All cyclic voltammetric studies were carried out using a PAR Model 362 scanning potentiostat/galvanostat with a Riken Denshi Model F5C *x-y* recorder. 50 ml of the electrolyte was taken in a plastic container and fitted with a cleaned platinum foil as a counter electrode. All measurements were made with respect to a Hg/HgO reference electrode containing the same electrolyte [10]. The potential of the Hg/HgO electrode is known to be independent of the hydroxyl ion concentration in the electrolyte [15] and this was found to be true in the 1–0.1 M range of electrolyte concentration in the present investigation. At higher concentrations slight changes were observed and the cyclic voltammograms suitably shifted. Thus the CVs presented in this study are directly comparable.

The switching potentials used throughout this study are 0.0 to +0.70 V for  $\text{Ni}(\text{OH})_2$  and –0.20 to +0.55 V for  $\text{Co}(\text{OH})_2$ . All measurements were performed at a scan rate of  $10 \text{ mV s}^{-1}$ . The anodic sweep was performed first, followed by the cathodic sweep in each cycle. Repetitive scans were made for each film until the peak positions attained a certain reproducibility in successive scans. In the case of  $\text{Ni}(\text{OH})_2$ , the peak positions became reproducible after the second scan, while in  $\text{Co}(\text{OH})_2$  reproducibility was estab-

Table 1. Results of cyclic voltammetry measurements of ES- $\text{Ni}(\text{OH})_2$  thin films in different electrolytes\*

Electrolyte		$E_{\text{anodic}}$ /mV	$E_{\text{cathodic}}$ /mV	$\Delta E_{\text{a,c}}$ /mV	$E_{\text{rev}}$ /mV	Coulombic efficiency† (%)
KOH	5 M	450	365	85	408	47
	1 M	450	365	85	408	61
	0.5 M	460	370	90	415	68
	0.1 M	520	375	145	448	81
	0.01 M	705	300	405	503	80
NaOH	1 M	440	350	90	395	64
	0.1 M	520	360	160	440	83
LiOH	1 M	450	365	85	408	50
	0.1 M	510	370	140	440	75
$\text{Ba}(\text{OH})_2$		480	350	130	415	69
$\text{Sr}(\text{OH})_2$		490	325	165	408	71
$\text{Ca}(\text{OH})_2$		510	300	210	405	86

\* All potentials are expressed with respect to a Hg/HgO reference.

† Evaluated as a ratio of the cathodic to anodic peak currents.

lished from the third scan. Thus, the fifth scans have been selected for detailed analysis in the present study.

A minimum of three fresh films were studied under every experimental condition to establish reproducibility of the film behaviour.

## 3. Results

Figures 1 and 2 show the cyclic voltammograms of  $\text{Ni}(\text{OH})_2$  and  $\text{Co}(\text{OH})_2$  films, respectively, in various alkali (1 M) and alkaline earth metal (saturated) hydroxide solutions. In the range of switching potentials employed both films showed one anodic and one cathodic peak. The difference in the anodic and cathodic peak positions,  $\Delta E_{\text{a,c}}$ , is taken as an estimate of reversibility of the reaction and the average potential is taken as an estimate of the reversible potential [12]. These estimates are tabulated in Tables 1 and 2.

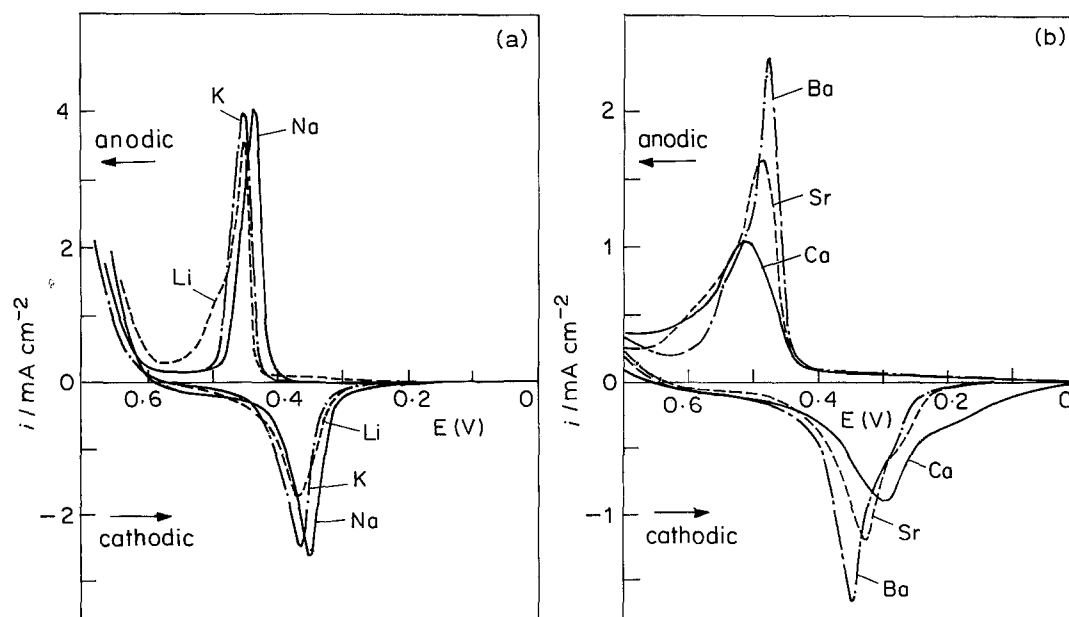


Fig. 1. CVs for  $\text{Ni}(\text{OH})_2$  thin films in different alkali (a) and alkaline earth (b) metal hydroxides.

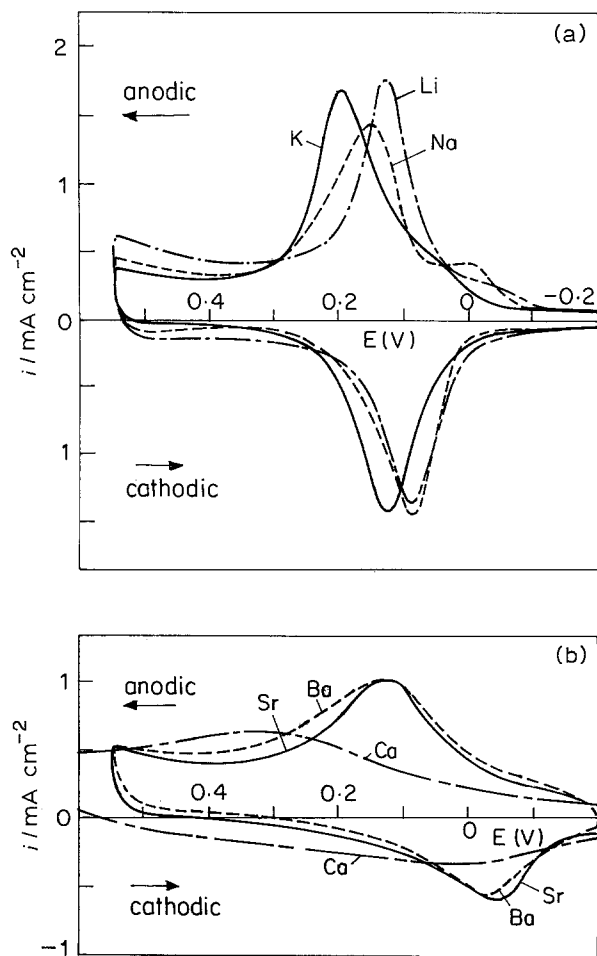


Fig. 2. CVs for  $\text{Co}(\text{OH})_2$  thin films in different alkali (a) and alkaline earth (b) metal hydroxides.

It is evident that the cathodic and anodic peak potentials of  $\text{Ni}(\text{OH})_2$  do not shift significantly in the three alkali metal hydroxides, but the coulombic efficiency in 1 M LiOH is decidedly less than in NaOH and KOH. In the alkaline earth hydroxides the anodic and cathodic peaks approach each other on going from Ca to Ba and also increase in intensity, suggesting a greater charge capacity and better reversible characteristics on going from Ca to Ba. The reversible

Table 2. Results of cyclic voltammetry measurements of  $\text{ES-Co}(\text{OH})_2$  thin films in different electrolytes\*

Electrolyte		$E_{\text{anodic}}$ /mV	$E_{\text{cathodic}}$ /mV	$\Delta E_{\text{a,c}}$ /mV	$E_{\text{rev}}$ /mV	Coulombic efficiency† (%)
KOH	1 M	200	125	75	163	80
	0.5 M	220	145	75	183	80
	0.1 M	290	160	130	225	80
	0.01 M	530	60	470	280	56
NaOH	1 M	150	90	60	120	95
	0.1 M	280	140	140	210	93
LiOH	1 M	125	90	35	108	76
	0.1 M	240	125	115	163	81
$\text{Ba}(\text{OH})_2$		125	-40	165	43	55
$\text{Sr}(\text{OH})_2$		125	-50	175	38	60
$\text{Ca}(\text{OH})_2$		310	-	-	-	-

\* All potentials are expressed with respect to a Hg/HgO reference.  
† Evaluated as a ratio of the cathodic to anodic peak currents.

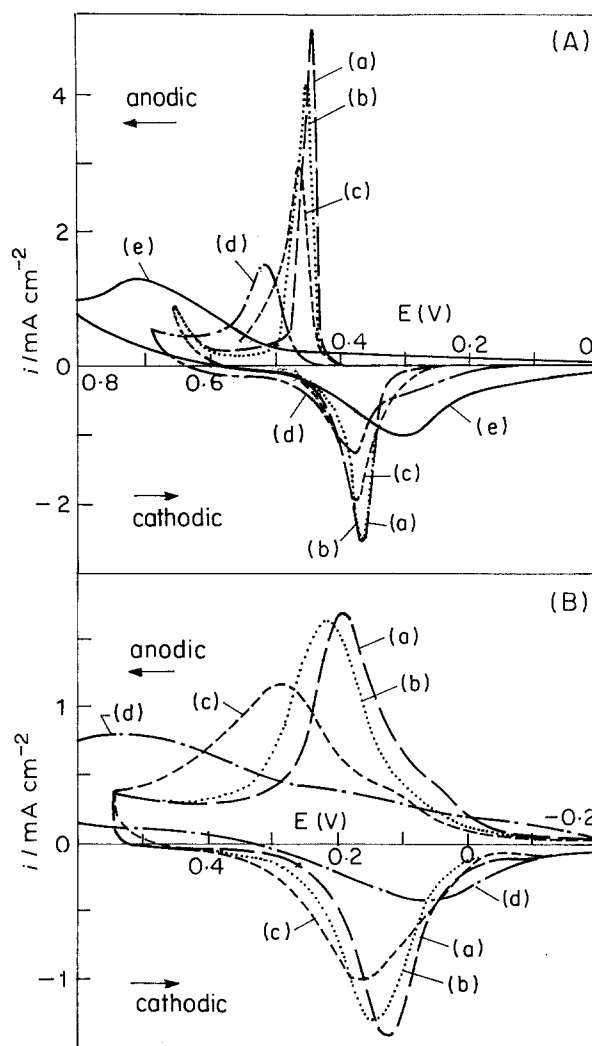


Fig. 3. (A) CVs for  $\text{Ni}(\text{OH})_2$  in KOH of different concentrations: (a) 5 M, (b) 1 M, (c) 0.5 M, (d) 0.1 M and (e) 0.01 M. (B) CVs for  $\text{Co}(\text{OH})_2$  in KOH of different concentrations: (a) 1 M, (b) 0.5 M, (c) 0.1 M and (d) 0.01 M.

potential in all the electrolytes remains nearly the same.

On the other hand  $\text{Co}(\text{OH})_2$  cyclic voltammograms show considerable cathodic shift on going from K to Li; the shift of the anodic peak (75 mV) is larger than the shift in the cathodic peak (35 mV). The reaction shows a greater degree of reversibility in LiOH ( $\Delta E_{\text{a,c}} = 35 \text{ mV}$ ) than in NaOH or KOH. In the alkaline earth hydroxides, the reaction is similar in Sr and Ba hydroxides, but is irreversible in  $\text{Ca}(\text{OH})_2$ .

Figure 3(a) and (b) show the effect of the electrolyte concentration on the cyclic voltammograms of  $\text{Ni}(\text{OH})_2$  and  $\text{Co}(\text{OH})_2$  by choosing KOH for the purpose of illustration. The electrolyte concentration has been varied from 5 to 0.01 M for  $\text{Ni}(\text{OH})_2$  and 1 to 0.01 M for  $\text{Co}(\text{OH})_2$ . It is seen that, in both cases, the anodic peak shifts to higher potentials on dilution of the electrolyte. The shifts are dramatic on going from 1 to 0.1 M and there is a decrease in the intensity of the peaks. Surprisingly, the changes in the cathodic peak positions are much less dramatic. In the case of  $\text{Ni}(\text{OH})_2$ , the cathodic peak position remains exactly the same in the 1–0.1 M range of electrolyte concentration for LiOH, NaOH and KOH (Fig. 4), while in

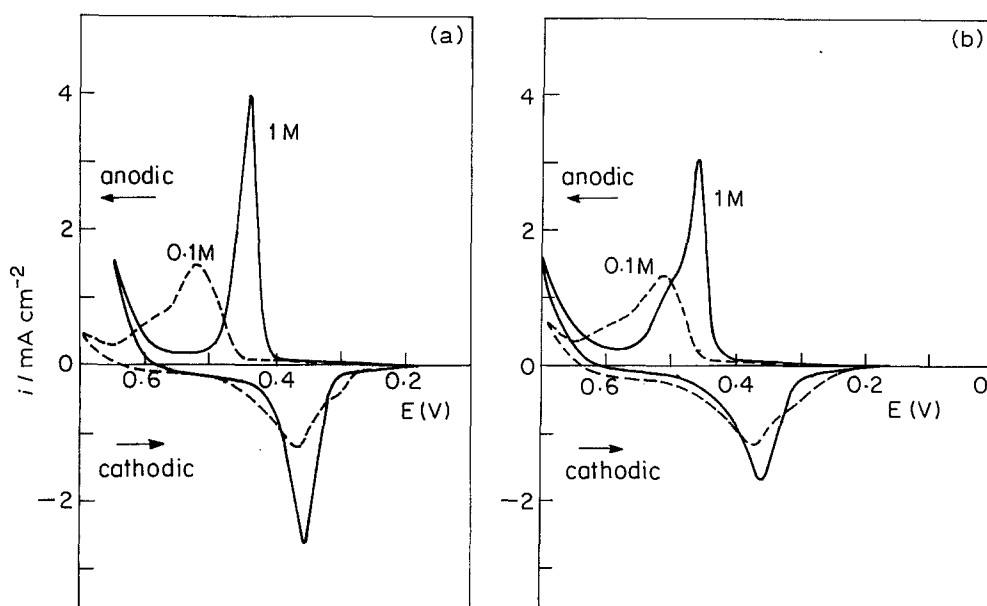


Fig. 4. CVs for Ni(OH)<sub>2</sub> in 1 M and 0.1 M concentrations of NaOH (a) and LiOH (b).

the case of Co(OH)<sub>2</sub> the anodic peak shifts (in the range of 130–90 mV) are much larger than the shift in the cathodic peak (35–50 mV) (Fig. 5). In other words, for both Ni(OH)<sub>2</sub> and Co(OH)<sub>2</sub>, the cathodic peak potential is less sensitive to the electrolyte concentration than the anodic peak potential. The reversible potential in all cases increases with dilution.

#### 4. Discussion

The cyclic voltammogram of Ni(OH)<sub>2</sub> shows only one anodic and one cathodic peak [1], although the reaction involves almost 1.7 oxidation state change for Ni [17]. Co(OH)<sub>2</sub>, on the other hand, undergoes a two step oxidation for a similar oxidation state change [9,18], but only a one step reduction. Thus, the first step ( $\text{Co}^{2+} \rightarrow \text{Co}^{3+}$ ) is irreversible, while the second step ( $\text{Co}^{3+} \rightarrow \text{Co}^{3.7+}$ ) is quasireversible. A Co(OH)<sub>2</sub>

electrode would be more akin to the MnO<sub>2</sub> electrode as it could be quasireversibly cycled between a nearly quadrivalent  $\text{H}_{0.3}\text{CoO}_2$  phase and a trivalent  $\text{HCoO}_2$  phase [9]. Discharge below  $\text{HCoO}_2$  does not take place and in this study; only the quasireversible reaction has been considered.

##### 4.1. Effect of electrolyte

ES-Ni(OH)<sub>2</sub> stabilizes in the  $\alpha$ -phase [1,16] with a large  $c$ -axis close to 0.8 nm, whereas ES-Co(OH)<sub>2</sub> goes into the rose-red  $\beta$ -phase with a much smaller  $c$ -axis of 0.46 nm on account of the inherent instability of the blue  $\alpha$ -phase. The larger  $c$ -axis of  $\alpha$ -Ni(OH)<sub>2</sub> understandably permits the free and facile incorporation of all alkali metal ions irrespective of their size, whereas their incorporation into  $\beta$ -Co(OH)<sub>2</sub> becomes increasingly difficult on going from Li<sup>+</sup> to K<sup>+</sup>, as reflected in the increase in  $E_{\text{rev}}$  from 108 mV (LiOH) to 163 mV (KOH), at a 1 M electrolyte concentration.

These effects are not clearly observed in the alkaline earth metal hydroxides, where dilution effects (to be discussed in the next section) probably outweigh the effects of ionic size. Ni(OH)<sub>2</sub> shows more reversible characteristics in barium hydroxide compared to Sr and Ca hydroxides. The irreversibility of the Co(OH)<sub>2</sub> reaction in calcium hydroxide and the small peak currents in Sr and Ba hydroxides show that, on the whole, the alkaline earth metal ions do not intercalate with the same ease as the alkali metal ions. The somewhat better reaction seen in the case of Ni(OH)<sub>2</sub> in barium hydroxide may be trivially related to its higher solubility compared to Sr and Ca hydroxides.

##### 4.2. Effect of the electrolyte concentration

On diluting the electrolyte,  $E_{\text{rev}}$  is found to shift to more positive potentials, in keeping with the observations of other authors [4,10] for Ni(OH)<sub>2</sub>. The same

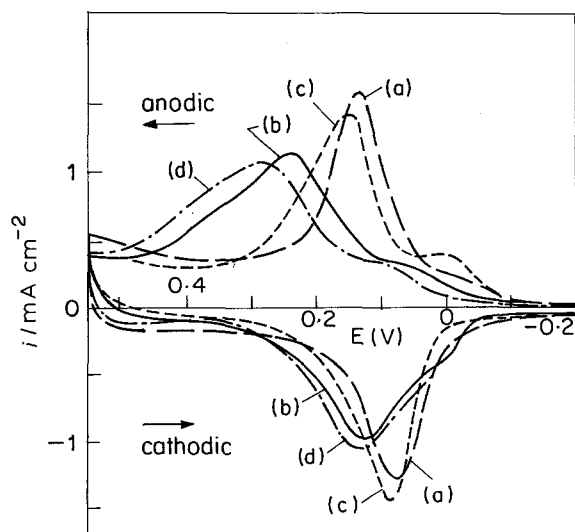


Fig. 5. CVs for Co(OH)<sub>2</sub> in 1 M and 0.1 M solutions of LiOH (a and b) and NaOH (c and d), respectively.

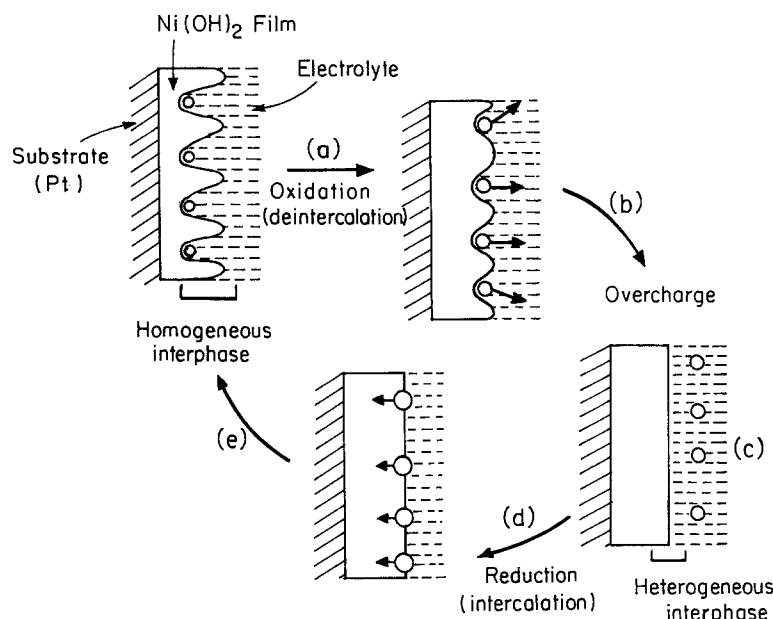


Fig. 6. Schematic model illustrating homogeneous deintercalation and heterogeneous intercalation of alkali metal ions (O) into a nickel hydroxide film (see text for details of steps (a) to (e)).

trends are also observed for  $\text{Co}(\text{OH})_2$ . There is also a decrease in the anodic and cathodic peak currents. While the fall in the peak currents upon electrolyte dilution can be attributed to the decreasing specific conductance of the electrolyte, the potential shifts arise for other reasons. It is specially significant that only the anodic peaks shift considerably, while the cathodic peaks remain constant or shift only marginally in the 1 to 0.1 M range of concentration. This leads to the possibility that the mechanism of oxidation is different from that of reduction, the latter being independent of the electrolyte concentration.

In the intercalation–deintercalation model [19], the driving force for the oxidation–reduction reactions of  $\text{Ni}(\text{OH})_2$  is provided by the reversible incorporation of alkali metal ions ( $\text{M}^+$ ) in the lattice. Oxidation takes place by deintercalation of  $\text{M}^+$  ions from the intersheet region of the layered material, while reduction takes place by incorporation of  $\text{M}^+$ . The present observation implies that deintercalation of  $\text{M}^+$  takes place homogeneously (see steps (a) and (b) in Fig. 6) across a nebulously defined, highly hydrated electrode–electrolyte interphase, somewhat akin to the hydrous oxide model of Burke [20]. When a sufficient number of  $\text{M}^+$  ions have been deintercalated from the intersheet region, the  $\gamma\text{-Ni}(\text{OH})$  phase is formed and separates from the parent material. This probably establishes a well defined heterogeneous interphase between the electrolyte and the electrode (see (c) in Fig. 6). In the reduction cycle (step (d) in Fig. 6),  $\text{M}^+$  is reincorporated across this heterogeneous interphase into the intersheet region of the electrode material. This reaction takes place at a potential independent of electrolyte concentration. When the electrode material has been sufficiently reduced, a homogeneous interphase is once again re-established with the  $\text{M}^+$  ions

from the electrolyte penetrating deep into the intersheet region of the electrode ((e) in Fig. 6).

A homogeneous charge–heterogeneous discharge model was earlier proposed by Barnard and others [21], but these authors did not take into consideration the crucial role played by the electrolyte in the process. This study, while providing direct evidence for the Barnard model, increases the scope of this model to include the role of the electrolyte. Similar conclusions also apply to the reactions of cobalt hydroxide.

## References

- [1] P. Oliva, J. Leonardi, J. P. Laurent, C. Delmas, J. J. Braconnier, M. Figlarz, F. Fievet and A. de Guilbert, *J. Power Sources* **8** (1982) 229.
- [2] J. Fitzpatrick and F. L. Tye, *J. Appl. Electrochem.* **21** (1991) 130.
- [3] P. V. Kamath and S. Ganguly, *Mater. Lett.* **10/11** (1991) 537.
- [4] D. M. MacArthur, *J. Electrochem. Soc.* **117** (1970) 422.
- [5] D. A. Corrigan and S. L. Knight, *ibid.* **136** (1989) 613.
- [6] C. Faure, Y. Borthomieu, C. Delmas and M. Fouassier, *J. Power Sources* **36** (1991) 113.
- [7] G. Feuillade and R. Jacoud, *Electrochim. Acta* **14** (1969) 1297.
- [8] J. Bauer, D. H. Buss, H. J. Harms and O. Glemser, *J. Electrochem. Soc.* **137** (1990) 173.
- [9] J. Ismail, M. F. Ahmed and P. V. Kamath, *J. Power Sources* **36** (1991) 505.
- [10] R. Barnard, C. F. Randell and F. L. Tye, *J. Appl. Electrochem.* **11** (1981) 517.
- [11] M. V. Vazquez, R. E. Carbonio and V. A. Macagno, *J. Electrochem. Soc.* **138** (1991) 1874.
- [12] D. A. Corrigan and R. M. Bendert, *ibid.* **136** (1989) 723.
- [13] K. C. Ho, *ibid.* **134** (1987) 52C.
- [14] D. A. Corrigan, *ibid.* **134** (1987) 377.
- [15] D. J. G. Ives, 'Reference Electrodes, Theory and Practice', Academic Press, New York (1961) pp. 322.
- [16] B. Mani and J. P. de Neufville, *J. Electrochem. Soc.* **135** (1988) 800.
- [17] J. Desilvestro, D. A. Corrigan and M. J. Weaver, *ibid.* **135** (1988) 885.
- [18] P. Benson, G. W. D. Briggs and W. F. K. Wynne-Jones,

- 
- Electrochim. Acta* **9** (1964) 275.
- [19] D. Fan and R. E. White, *J. Electrochem. Soc.* **138** (1991) 2952.
- [20] L. D. Burke and M. E. G. Lyons, 'Modern Aspects of Electrochemistry 18', (edited by R. E. White and others), Plenum Press, New York (1986) pp. 169.
- [21] R. Barnard, C. F. Randell and F. L. Tye, *J. Appl. Electrochem.* **10** (1980) 109.